Title

Soil Moisture Stress as a Major Driver of Carbon Cycle Uncertainty

Journal

Geophysical Research Letters, 45(13)

ISSN

0094-8276

Authors

Trugman, AT
Medvigy, D
Mankin, JS
et al.

Publication Date

2018-07-16

DOI

10.1029/2018gl078131

Peer reviewed

Geophysical Research Letters

RESEARCH LETTER
10.1029/2018GL078131

Key Points:
- Most global vegetation models represent plant water limitation with a rarely tested empirical function based solely on soil moisture
- Carbon cycle uncertainty associated with such soil moisture stress functions is comparable to current global gross primary productivity
- Forty to eighty percent of the soil water stress-driven uncertainty in productivity among models is due to the functional form of the stress equation alone

Supporting Information:
- Supporting Information S1

Correspondence to:
A. T. Trugman,
a.trugman@utah.edu

Citation:
Trugman, A. T., Medvigy, D., Mankin, J. S., & Anderegg, W. R. L. (2018). Soil moisture stress as a major driver of carbon cycle uncertainty. *Geophysical Research Letters*, *45*, 6495–6503. https://doi.org/10.1029/2018GL078131

Received 28 MAR 2018
Accepted 8 JUN 2018
Accepted article online 19 JUN 2018
Published online 6 JUL 2018

Soil Moisture Stress as a Major Driver of Carbon Cycle Uncertainty

A. T. Trugman[1], D. Medvigy[2], J. S. Mankin[3,4], and W. R. L. Anderegg[1]

[1]Department of Biology, University of Utah, Salt Lake City, UT, USA, [2]Department of Biological Sciences, University of Notre Dame, Notre Dame, IN, USA, [3]Division of Ocean and Climate Physics, Lamont-Doherty Earth Observatory of Columbia University, Palisades, NY, USA, [4]Department of Geography, Dartmouth College, Hanover, NH, USA

Abstract Future projections suggest an increase in drought globally with climate change. Current vegetation models typically regulate the plant photosynthetic response to soil moisture stress through an empirical function, rather than a mechanistic response where plant water potentials respond to changes in soil water. This representation of soil moisture stress may introduce significant uncertainty into projections for the terrestrial carbon cycle. We examined the use of the soil moisture limitation function in historical and future emissions scenarios in nine Earth system models. We found that soil moisture-limited productivity across models represented a large and uncertain component of the simulated carbon cycle, comparable to 3–286% of current global productivity. Approximately 40–80% of the intermodel variability was due to the functional form of the limitation equation alone. Our results highlight the importance of implementing mechanistic water limitation schemes in models and illuminate several avenues for improving projections of the land carbon sink.

Plain Language Summary Understanding the environmental controls of terrestrial ecosystem productivity is of critical importance because terrestrial ecosystems directly impact the concentration of CO_2 in the atmosphere. However, model projections disagree on the future sign and magnitude of terrestrial ecosystem CO_2 drawdown, so it is uncertain if terrestrial ecosystems will continue to mitigate climate change in the future. Here we show that the current representation of water-limited productivity across state-of-the-art vegetation models is a large and uncertain component of terrestrial productivity, comparable in magnitude to current global productivity. Our results provide a foundation for improved projections of climate change impacts on terrestrial ecosystems, ranging from vegetation growth to agricultural productivity.

1. Introduction

Terrestrial ecosystems currently sequester ~2.4 Pg C annually (Pan et al., 2011), but their ability to maintain these sequestration rates is uncertain and depends on potentially compensating impacts of both CO_2 fertilization and increased hydrologic stress (Allen et al., 2015). A number of regional observational studies have attributed recent declines in forest growth and increases in mortality over a wide range of latitudes to climate change-induced drought stress (Allen et al., 2010; Brienen et al., 2015; Trugman et al., 2018; van Mantgem et al., 2009). Yet global estimates observe an overall strengthening of land carbon uptake (Ballantyne et al., 2012), gross primary productivity (GPP; Campbell et al., 2017), vegetation leaf area (Zhu et al., 2016), and plant water use efficiency (Keeling et al., 2017) over the past several decades. Process-based global vegetation models (VMs), either run offline or incorporated into Earth system models (ESMs), are a practical tool for bridging this scaling gap and understanding the response of terrestrial ecosystems to changes in atmospheric CO_2 and climate, but such VMs must include the appropriate physiological mechanisms for them to be useful for this purpose.

Current estimates project an increase in the land carbon sink over the next century due mainly to CO_2 fertilization (Friend et al., 2014; Huntingford et al., 2013; Sitch et al., 2015). However, predictions vary widely depending on both VM (Friedlingstein et al., 2014; Friend et al., 2014; Sitch et al., 2015) and climate model (Huntingford et al., 2013). The large intermodel variability highlights the need for a better understanding of the water stress mechanisms incorporated into VMs. This need is urgent given that water stress is projected to increase and soil moisture is projected to decrease in many regions under all emissions scenarios (Berg et al., 2016; Dai et al., 2004; Sheffield & Wood, 2007).

Most global VMs have simplistic representations of the effects of soil water stress on vegetation growth over long time scales (Powell et al., 2013). In many cases, either photosynthesis or stomatal conductance is downregulated using an empirical function (β) that ranges between 0 and 1, with $\beta = 0$ analogous to full stomatal closure due to soil moisture limitation. β is generally dependent on available soil moisture and root distribution, and the functional form of β varies between models (supporting information Text S1). Several significant shortcomings result from this representation of plant hydraulic stress: First, β does not capture widely documented differences in vulnerability to soil moisture stress across plant species, heights, or functional types (Xu et al., 2016). Second, the use of β in models decouples the plant water potential response to atmospheric vapor pressure deficit (VPD; Ball et al., 1987) from the plant soil moisture stress response. This representation of plant water stress is unlikely to capture the complex and nonlinear interactions between soil water potential and VPD that affect stomatal conductance through the influence on leaf water potential (Sperry et al., 2016). Third, the effects of different β functions have generally not been evaluated against empirical data or compared across models, and thus their influence on simulated terrestrial carbon dynamics is largely unknown. Most importantly, lacking a mechanistic grounding, β may not accurately capture ecosystem response to water stress (Powell et al., 2013), and thus increasing β-constrained GPP with climate change could introduce significant uncertainty into future projections of the terrestrial carbon cycle.

We quantified the prevalence of β use in historical and the Representative Concentration Pathway (RCP) 8.5 future emissions scenarios in nine ESMs used in the Coupled Model Intercomparison Project, Phase 5 (CMIP5). Collectively, the models used seven different β functions, seven unique soil grids, and four different spatial resolutions (Table S1). β was not archived as a standard CMIP5 output, so we calculated its average value using monthly-level soil moisture, the known β functional form (Table S1), and soil texture from the Global Soil Wetness Project 2 (Dirmeyer et al., 2002). Additionally, all models except the MIROC-ESM (Sato et al., 2007) require root biomass for each soil layer to calculate β. Root biomass by soil layer is not available in the CMIP5 archive, so we instead used established curves for rooting depth based on Jackson et al. (1996). A validation of this inversion approach against direct model output of β and sensitivity analyses on inputs to the inversion approach are available in the supporting information Texts S1–S6. In each model, we further calculated the maximum amount that the derived β could constrain potential GPP (referred to as GPP_c) according to the following relation:

$$\mathrm{GPP}_c = \mathrm{GPP}_m \times \left(\frac{1}{\max(\beta, 0.1)} - 1 \right). \quad (1)$$

In equation (1), GPP_m is the model output GPP. $\mathrm{GPP_c}$ is designed to quantify first-order uncertainty in estimates of productivity constrained by β where $\mathrm{GPP_m}$ + $\mathrm{GPP_c}$ ~ potential GPP. Note, however, that $\mathrm{GPP_c}$ should not be interpreted as the GPP that *could have been supported* without β because it does not include land-atmosphere feedbacks (i.e., the influence of vegetation productivity on surface energy fluxes and the hydrological cycle, and the subsequent feedbacks on climate and future vegetation productivity). We asked the following: (i) What are the global patterns of β and in what regions does β constrain potential GPP? (ii) Is the average β lower in RCP 8.5 (i.e., more water stress) compared to historical simulations? (iii) Is intermodel variation due mainly to variation in the functional form of β or variation in other model structures and/or climate? (iv) How large is the uncertainty in $\mathrm{GPP_m}$ due to $\mathrm{GPP_c}$ and what are the drought implications for terrestrial carbon cycle uncertainty?

2. Materials and Methods

2.1. Soil Moisture Limitation in CMIP5 Simulations

We obtained soil moisture at the monthly time scale from historical runs and RCP 8.5 from the CMIP5 multimodel ensemble archive available at the Centre for Environmental Data Archival (https://services.ceda.ac.uk/) for one realization for each of nine models—BCC-CSM1-1, BNU-ESM, CanESM2, CCSM4, CESM1-BGC, GISS-E2-R-CC, HadGEM2-ES, MIROC-ESM, and NorESM1-ME. Only one realization was used in this analysis because the soil moisture equation used to limit photosynthesis (β) is a product of model structure rather than initial conditions. However, using only one realization neglects possible multidecadal variability in soil moisture between different model realizations. To avoid confounding short-term variability in soil moisture and $\mathrm{GPP_m}$, we computed the average soil moisture for each model for each month over the

period from 1981 to 2000 and from 2080 to 2099 for the historical and RCP 8.5 simulations, respectively. For ease of comparison, model output was regridded to a 1° grid and the soil column was regridded to the CCSM4 grid that extends through 4.7 m. Our regridding calculations were performed in MATLAB using a nearest neighbor method from the *interp* function to preserve the spatial distribution of soil moisture as best as possible for each individual model.

The functional form of β generally requires a metric of soil moisture, soil field capacity, and soil wilting point (supporting information Text S1). Thus, we downloaded global maps at 1° resolution of volumetric soil water content at saturation, wilting point, and field capacity as well as soil water potential at saturation, and rooting depth encompassing 50% of root biomass from the GWSP2 database (Dirmeyer et al., 2002), a soil texture database used in a number of Earth system models (Sato et al., 2007). We further calculated soil water potential at field capacity and wilting point using the Clapp-Hornberger equation and downloaded soil parameters from the GWSP2. Additionally, all models except the MIROC-ESM (Sato et al., 2007) require the amount of root biomass in each soil layer. This output was not available for individual models in the CMIP5 archive, so we instead calculated the root biomass fraction in each soil layer by fitting an established rooting depth curve from Jackson et al. (1996; one of the primary references from which global vegetation root distribution are based on VMs; Zeng, 2001) to the 50% root biomass fraction from the GWSP2 database. Finally, we masked out all locations covered in ice year-round circa year 2000. After post-processing, we averaged monthly-level values of β over the year for both the historical and RCP 8.5 simulations to obtain two global maps of β for comparison with each model, one representing average conditions circa 2000 and one circa 2100.

2.2. Estimated Impacts of Soil Moisture Limitation on Simulated GPP

We downloaded average daily minimum temperature and GPP, averaged to the monthly scale, from historical runs and RCP 8.5. For NorESM1-ME only, we used average monthly temperature rather than average daily minimum temperature because daily minimum temperature was not available. We processed and regridded these model outputs in the same manner as soil moisture. Because we were interested in examining the water limitation impact of β on GPP, we masked out GPP during months when average minimum temperature decreased below 273.15 K.

We then calculated the simulated global GPP (GPP_m) that was reduced by β (GPP_c) in each model according equation (1). For numerical purposes, in our calculation of GPP_c, we limited the minimum value of β to 0.1. Though in some models β is used to regulate the maximum rate of photosynthesis and in others it is used to regulate canopy conductance (supporting information Text S1), GPP_m scales roughly linearly with β in either case and we treated both identically in our first-order estimates of GPP_c. After obtaining estimates of monthly-level GPP_c, we summed monthly-level values during the growing season over the year for both the historical and RCP 8.5 simulations to obtain global maps of GPP_c (using β functions associated with their own respective CMIP5 model) for average conditions circa 2000 and circa 2100. To quantify the effect that different β functions used across models has on GPP_c, we applied all seven different β equations (supporting information Text S1) to a single model's soil moisture output. We compared the variability in globally integrated β for a given model soil moisture using the seven different β functions to the variability in globally integrated β across models (each with their own model-specific β function) to attribute the first-order variability in β and GPP_c associated with the functional form of the β equation alone, thus enabling a better understanding the role of β in carbon cycle uncertainty.

2.3. Validations of Soil Moisture Limitation Estimates

In this study, β was calculated via inversion using model output soil moisture, assumed root biomass curves (for all models except the MIROC model), assumed soil hydraulic parameters, and assumed soil moisture variability at a monthly time scale. We validated the inversion approach using monthly average β calculated directly with a fully coupled simulation of the CESM model (supporting information Text S2). We used this information to assess whether our inversion approach to obtaining β is a reasonable proxy in estimating β strength and spatial distribution for models with β dependent on root biomass. For the MIROC model, β is calculated exclusively from soil moisture and so is analogous to our estimates (supporting information Text S1). We found that in using the inversion approach, we were able to capture both the spatial variability and strength of β.

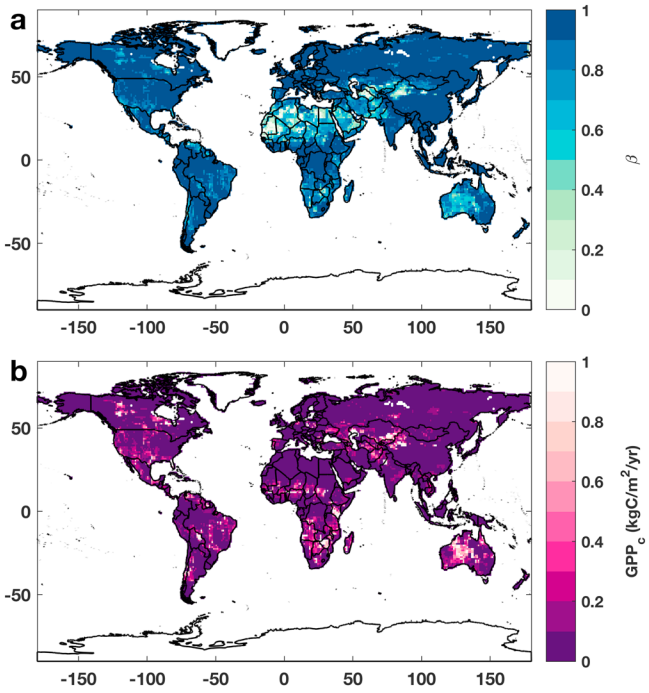

Figure 1. Regions with projected soil moisture limitation on photosynthesis comprise a large portion of the land surface area in vegetation models. Global maps of the multimodel median (a) soil water limitation coefficient (β) and (b) GPP constrained by β (GPP_c). Maps show the average annual β and GPP_c (using β functions associated with their own respective model) over the years 2080–2099 for RCP 8.5 for nine model members of the CMIP5 (Table S1). GPP = gross primary productivity; RCP = Representative Concentration Pathway; CMIP5 = Coupled Model Intercomparison Project, Phase 5.

In a separate analysis, we applied the soil moisture stress function to individual months in each 20-year period and then computed the mean monthly β, given that β is sometimes a nonlinear function of soil moisture levels. Our calculations using monthly soil moisture instead of climatological soil moisture led to slightly lower values of β - particularly in semiarid areas (e.g., South Africa and central United States; see supporting information Text S3 for details). Thus, the climatological results presented in the main text are actually a conservative estimate of β stress and GPP_c in some regions.

Finally, we quantified the sensitivity of our results to assumptions for plant rooting depth and timescale of analysis (supporting information Text S4–6).

2.4. Feedback of Soil Water Stress Factor (β) on GPP in an Earth System Model

Soil moisture stress is not the only water stress that can impact plant productivity. High atmospheric VPD stress can also decrease GPP through a downregulation of stomatal conductance. Further complicating this is the fact that low soil moisture is often correlated with high VPD in a number of locations. In this case, the inversion method for estimating GPP_c from β could overestimate GPP_c as VPD-induced stomatal closure would further constrain GPP, thus confounding our estimate of GPP_c. To disassociate these two drivers, we performed a novel set of two 20-year, fully coupled Earth system model integrations: one *with* and one *without* the soil moisture (β) effect on GPP under high greenhouse gas emissions (years 2080–2100 in RCP8.5) for the CESM model only (model #5 in Table S1). In the test simulation we turned β off (i.e., set β = 1, which represents no soil water stress) for land areas that do not have ice cover, removing soil moisture stress from influencing GPP. In this test simulation, we increased the error tolerance that conserves the land surface water budget in CESM because β is critical to maintaining the water budget in the CESM model. We compared the test ($\beta = 1$) simulation to a control simulation where β was allowed to respond to soil water and root resistances. We then calculated the simulated average annual difference in GPP (GPP_{diff}) between the fully coupled test simulation ($\beta = 1$) from the control simulation over the years 2080–2099. It should be noted that GPP_{diff} is not analogous to GPP_c. GPP_c is defined as the uncertainty associated with GPP due to the model β parameterization, whereas GPP_{diff} is the change in GPP without β but including land-atmosphere feedbacks on GPP.

3. Results and Discussion

3.1. Global Patterns in β and GPP_c

Values of β were smallest (hereafter *strongest* water limitation) in RCP 8.5 in the desert regions. In northern and parts of southern Africa, the Arabian Peninsula, central Asia, and much of Australia, extensive portions of the land area had photosynthesis suppressed by 40% ($\beta \sim 0.6$; Figure 1a). Substantial portions of Central America, the Brazilian Cerrado, Argentina, and the American West experienced $\beta \sim 0.7$. However, individual models varied significantly, and some projected much stronger β signals than others (Figures S1a, S1b, and S2).

Patterns of GPP_c differed from those of β due to the relationship between β and GPP_m (Figure 1b). Specifically, desert regions with extremely water-stressed photosynthesis had minimal GPP_m, diminishing the importance of strong β values there. However, semiarid grassland and savanna regions under moderate β stress had a much higher total GPP_m, and in these locations GPP_c exceeded 0.2 kg $C{\cdot}m^{-2}{\cdot}year^{-1}$ for relatively large regions and 0.8 kg $C{\cdot}m^{-2}{\cdot}year^{-1}$ at smaller scales (Figure 1b), a substantial fraction of the multimodel median GPP_m of ~0.5–2 kg $C{\cdot}m^{-2}{\cdot}year^{-1}$ for similar regions. Additionally, the large intermodel variation in β globally resulted in considerable variability in GPP_c (Figures S1c, S1d, and S3), due to both intermodel

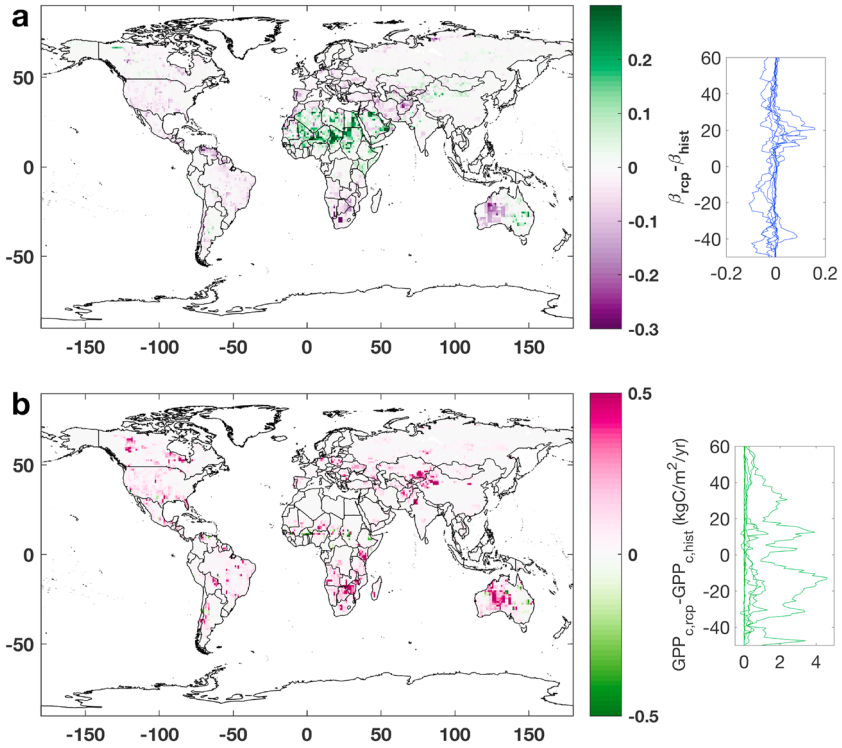

Figure 2. Drought limitation on photosynthesis is projected to increase in the future; however, substantial spatial variability in the strength and extent is apparent. Global maps of the multimodel median difference in (a) soil water limitation coefficient (β) and (b) GPP constrained by β (GPP_c). Maps show the median annual β and GPP_c over the years 2080–2099 for RCP 8.5 minus the median for years 1981–2000 in historical simulations for nine model members of the CMIP5 (Table S1). Side panels illustrate zonal means for individual models. See Figure S6 for the corresponding individual models. GPP = gross primary productivity; RCP = Representative Concentration Pathway; CMIP5 = Coupled Model Intercomparison Project, Phase 5.

variation in β and GPP_m (Figures S2 and S3). Semiarid regions have been identified as a major source for variability in the land carbon sink in ecosystem models (Ahlström et al., 2015; Poulter et al., 2014). This could be partially attributable to the relatively strong β stress across semiarid regions in models.

3.2. Future Changes in β and GPP_c

Plant water limitation increased globally between 2000 and 2100 in all models. Median β decreased on average by ~0.003, corresponding to a median increase in average GPP_c by ~0.088 kg C·m^{-2}·year^{-1} due to both decreased soil moisture and increased GPP_m from atmospheric CO_2 fertilization (Figure 2). Notably, β increased at ~20°N due to a moistening of the Sahel in most models (Figures 2a and S4). However, a number of regions with moderate to high productivity, particularly in South America, experienced decreases in β due to projected decreases in soil moisture (Figure S4). These regional decreases in β in productive areas corresponded to substantial increases in GPP_c (Figures 2b and S5).

Collectively, the future changes in GPP_c intimate at the potential utility of β and GPP_c as complementary metrics of monthly scale drought. Much of the drought impacts literature is concerned with the appropriateness of present-day drought measures to assess future drought risks (Mankin et al., 2017; Milly & Dunne, 2016; Roderick et al., 2015; Swann et al., 2016; Trenberth et al., 2013). By contrast, the estimation of β is (1) internally consistent within each model between historical and future climates and (2) is directly relevant to plant water stress and simulation of global carbon and water fluxes. Thus, the combined use of β and GPP_c gives both the physiological (β) and carbon cycle (GPP_c) relevance of projected changes in water stress. Our results for projected changes in β show a systematic increase in physiological water stress in future projections in regions where there is moderate to high productivity such as South America. Though there is substantial intermodel variability, there is a routine decrease in water stress (increase in β) in drier locations such as the Sahel and a

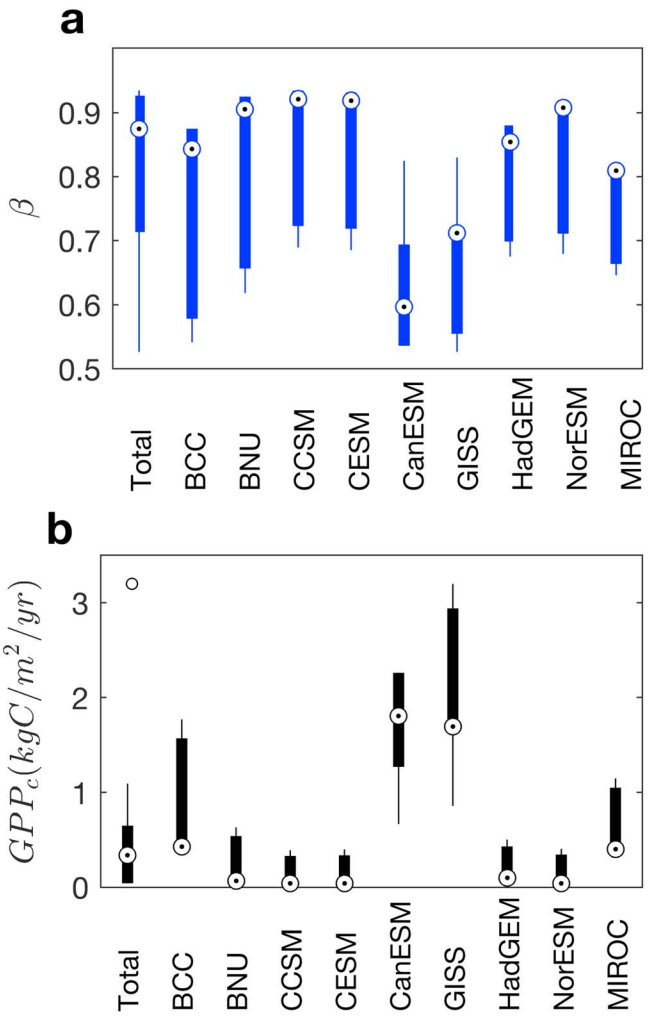

Figure 3. Variation in the functional form of the soil water limitation coefficient contributes to the large uncertainty in soil moisture-constrained GPP. Intermodel and intramodel variability in the global average (a) soil water limitation coefficient (β) and (b) GPP constrained by β (GPP_c) for RCP 8.5 future projections. In both panels, we computed the intermodel range for each model given its own β function (*Total*; Table S1) and the intramodel range for each model given the range of the seven β functions applied to individual model-predicted soil moisture and GPP (supporting information Text S1). Central dots indicate the median model value; thick bars define the interquartile range; thin lines represent 2.7 standard deviations; open circles indicate outliers. GPP = gross primary productivity; RCP = Representative Concentration Pathway.

routine increase in water stress (decrease in β) in much of South America, Europe, West Asia, and parts of North America (Figures 2 and S4). Both the decrease in β and the increase in GPP_m lead to a substantial increase in GPP_c that can be threefold to fourfold, depending on the model and location (Figure S5). These results indicate that despite decreased productivity due to physiological response to increased water stress circa 2100, gains in productivity associated with CO_2 fertilization may compensate for the increased physiological stress. However, an increase in uncertainty in future carbon cycle projections (i.e., an increase in GPP_c) is concomitant with both increased water stress and increased GPP_m.

3.3. The β, GPP_c, and Terrestrial Carbon Cycle Uncertainty

Both the functional form of β and variability in soil moisture between models contributed to the large intermodel variation in global average β. When β was calculated for individual models circa 2100, the global median β ranged from ~0.6 to 0.9 (Figure 3a). However, when we applied the range of β functional forms (supporting information Text S1) to soil moisture output from a given model, the global median β often varied by ~0.2 and up to ~0.3 with lower values of β corresponding to β functions using soil moisture and higher values corresponding to β functions using soil water potential. This variability in the intramodel range in global mean β, given the seven β functions, was due to variability in model-predicted soil moisture (Figure 3a).

Next, we quantified how variability due solely to the functional form of β affected GPP_c. In many models, we found that GPP_c varied by ~0.3–0.5 and up to ~2 kg C·m^{-2}·year^{-1} (Figure 3b). Further, we found that the functional form of β alone explained ~40–80% of the intermodel variance in soil moisture stress on vegetation productivity (GPP_c), indicating that β variability among models could be a substantial source of intermodel variation documented for projected changes in land productivity (Friedlingstein et al., 2014).

GPP_c represented a large and uncertain term relative to other components of the projected terrestrial carbon budget for all models. In the historical simulations, total GPP_c ranged from 4.0 to 353.0 Pg C year^{-1} with a median of 34.7 Pg C year^{-1} (Figures 4a and 4b). For context, GPP_c is of the same magnitude as observation-based estimates of total GPP (123 ± 8 Pg C year^{-1}; Beer et al., 2010) and GPP_m (Figure S7a), and 0.4- to 36-fold larger than annual fossil fuel emissions for 2014 (9.8 Pg C year^{-1}; Le Quéré et al., 2015; Figure 4a). In the RCP 8.5 simulations, total GPP_c ranged from 5.56 to 595.5 Pg C/year with a median of 64.2 Pg C year^{-1} (Figures 4c and 4d). In some cases, future projected GPP_c exceeded model-based projections of GPP (Mystakidis et al., 2016; Figure S7b) and was roughly equivalent to projected fossil fuel emissions (29 Pg C year^{-1}) in the highest emissions scenario (Sanford et al., 2014; Figure 4c). For both historical and future projections, GPP_c was of the same magnitude as nitrogen-constrained GPP (Thornton et al., 2007). Depending on model and time period, GPP_c was equivalent to 3–286% of GPP_m (Figure S7b). This increase in GPP_c globally was attributable to both increased water limitation in moderately to highly productive regions (depending on the model; Figure S4) and an increase in total global productivity (Figure S7).

3.4. Caveats

Vegetation in regions exposed to high VPD stress also experiences decreased GPP through a downregulation of stomatal conductance. Thus, VPD stress could result in an overestimate of GPP_c because GPP constrained by VPD-induced stomatal closure would be included our calculation of GPP_c. However, an Earth system

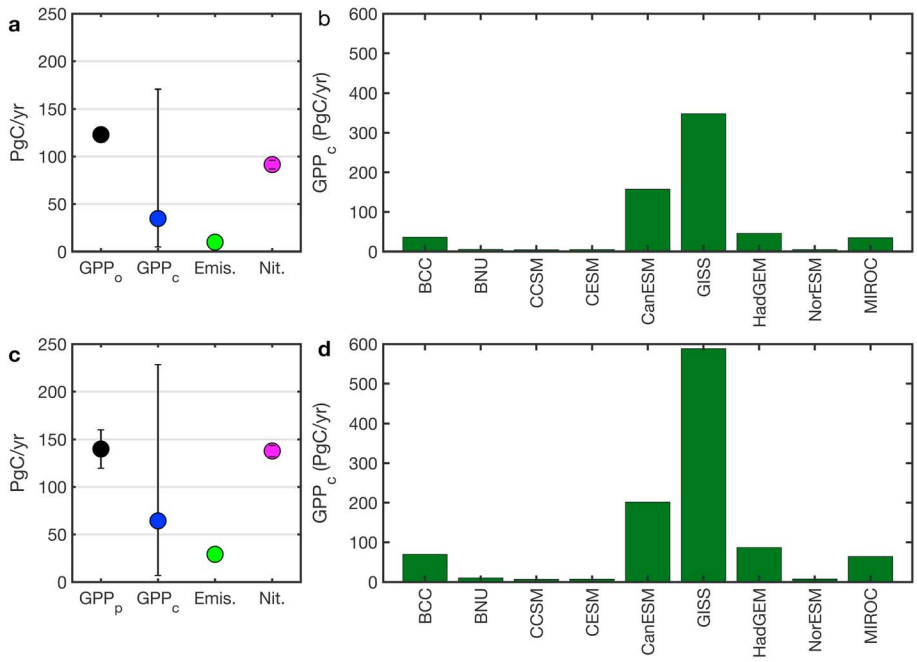

Figure 4. GPP constrained by soil water limitation represents a key uncertainty in the terrestrial carbon cycle, comparable in magnitude to global GPP. (a) Historical GPP constrained by soil water stress (GPP_c) compared to observation-based estimates of GPP (GPP_o), global CO_2 emissions (Emis.) in 2014, and GPP constrained by nitrogen limitation (Nit.), and (b) individual model GPP_c. (c) Projected GPP_c compared to projected GPP (GPP_p), projected global CO_2 emissions, and GPP constrained by nitrogen limitation, and (d) individual model GPP_c. Panels (a) and (c) show model median and range between the 0.159 and 0.841 quantiles for GPP_c and mean ± 1 standard deviations for GPP_o and GPP_p. Calculations of GPP_c were performed using β functions associated with their own respective model. GPP = gross primary productivity.

simulation with freely varying β relative to a simulation with no β influence ($\beta = 1$, section 2.4) shows patterns of substantially decreased GPP globally and particularly in arid and semiarid regions where high VPD regulates photosynthesis (Figure S8). These simulations illustrate that there is a meaningful downregulation of GPP by β, regardless of VPD downregulation of photosynthesis. Overall, these simulations provide an estimate of the soil moisture effect on GPP independent of GPP regulation by atmospheric VPD, and they further validate the potential for β to propagate substantial uncertainty in model estimates of terrestrial GPP.

4. Conclusions

Collectively, these results illustrate that soil moisture stress on photosynthesis is a large and uncertain term affecting estimates of the terrestrial carbon cycle, comparable in magnitude to observed estimates of global GPP, simulated GPP_m, and the effects of nitrogen limitation on photosynthesis. These results also highlight several avenues for improving the representation of (a) soil hydraulic processes and (b) water limitation on photosynthesis. We found substantial intermodel variability in soil moisture, which resulted in a large intermodel variation in β globally (Figures 3a and S1–S3). Models with lower soil moisture (CanESM2, GISS-E2-R-CC, and HadGEM2-ES; Figure S2) also exhibited a wider variability in β due to the functional form alone (Figure 3a). Drier soils in models were associated with coarser-resolution soil grids within the rooting zone (Table S1). It has already been recognized that soil column depth and resolution is crucial in capturing permafrost dynamics (Lawrence et al., 2008). Our results indicate that increased vertical resolution may also be important in capturing the impacts of soil moisture stress on the terrestrial carbon cycle.

These results indicate that the β soil moisture scheme is responsible for ~40–80% of the intermodel variability in GPP_c, indicating that the β parameterization is likely an important mechanism responsible for the large intermodel spread in carbon cycle projections, particularly in semiarid ecosystems. Specifically, the practice of tuning individual models to historical observations of GPP, given model-specific β equations and other

processes, likely results in compensating errors that manifest themselves as diverging future projections in the carbon cycle. These results provide a unique and important rationale and guidance for a broad audience of scientists working to improve the representation of hydrologic stress in global vegetation models, as well as many of the more detailed uncoupled models that also use a simple soil moisture stress scheme similar to β. Further, such β-induced carbon cycle uncertainties likely influence hydrologic uncertainties, as CO_2-fertilized vegetation siphons water from both runoff and soil moisture in Earth system models over some ~40% of the globe, notably in semiarid regions (Mankin et al., 2017, 2018). Trait-driven representations of water limitation, whereby leaf and stem water potential are explicitly resolved and used to estimate root zone water uptake, transport of water vertically through the sapwood, and transpiration of water into the atmosphere, are beginning to be used by the modeling community (Christoffersen et al., 2016; Trugman et al., 2016; Xu et al., 2016). Recent studies also indicate that including water stress-induced loss of living carbon, such as sapwood used for water transport (Shevliakova et al., 2009), may allow VMs to better capture drought legacy effects on growth (Anderegg et al., 2015). These findings motivate consistent, process-based representations of water limitation in all VMs as a fundamental component to our ability to accurately capture impacts of water limitation on the terrestrial carbon cycle with global climate change.

Acknowledgments

The authors declare no conflict of interest. We acknowledge the World Climate Research Programme's Working Group on Coupled Modeling, which is responsible for CMIP, and we thank the climate modeling groups (listed in the supporting information) for producing and making available their model output. The authors acknowledge support from the USDA National Institute of Food and Agriculture Postdoctoral Research Fellowship grant 2017-07164 to A. T. T.; the National Science Foundation grant 1714972, the University of Utah Global Change and Sustainability Center, and the USDA National Institute of Food and Agriculture, Agricultural and Food Research Initiative Competitive Programme, Ecosystem Services and Agro-ecosystem Management, grant 2017-05521 to W. R. L. A.; National Science Foundation Award 1151102 and U.S. Department of Energy, Office of Science, Office of Biological and Environmental Research, Terrestrial Ecosystem Science (TES) Program award DE-SC0014363 to D. M.; and the Earth Institute to J. S. M. We also thank Steve Pacala for his helpful feedback. Lamont Contribution 8228. All CMIP5 multimodel ensemble data are available at the Centre for Environmental Data Archival (https://services.ceda.ac.uk/). Maps of estimated β and GPP_c are archived on the Hive, the University of Utah's Open Access Institutional Data Repository (https://hive.utah.edu/concern/generic_works/pk02c973d; doi:10.7278/S5707ZMS).

References

Ahlström, A., Raupach, M. R., Schurgers, G., Smith, B., Arneth, A., Jung, M., et al. (2015). The dominant role of semi-arid ecosystems in the trend and variability of the land CO_2 sink. *Science*, *348*(6237), 895–899. https://doi.org/10.1126/science.aaa1668

Allen, C. D., Macalady, A. K., Chenchouni, H., Bachelet, D., McDowell, N., Vennetier, M., et al. (2010). A global overview of drought and heat-induced tree mortality reveals emerging climate change risks for forests. *Forest Ecology and Management*, *259*(4), 660–684. https://doi.org/10.1016/j.foreco.2009.09.001

Allen, C. D., Breshears, D. D., & McDowell, N. (2015). On underestimation of global vulnerability to tree mortality and forest die-off from hotter drought in the Anthropocene. *Ecosphere*, *6*(8), 129. https://doi.org/10.1890//ES15-00203.1

Anderegg, W. R., Schwalm, C. R., Biondi, F., Camarero, J. J., Koch, G., Litvak, M., et al. (2015). Pervasive drought legacies in forest ecosystems and their implications for carbon cycle models. *Science*, *349*(6247), 528–532. https://doi.org/10.1126/science.aab1833

Ball, J. T., Woodrow, I. E., & Berry, J. A. (1987). In J. Biggins (Ed.), *A model predicting stomatal conductance and its contribution to the control of photosynthesis under different environmental conditions BT - Progress in photosynthesis research: Volume 4 Proceedings of the VIIth International Congress on Photosynthesis Providence, Rhode Island, USA, August 10–15, 1986* (pp. 221–224). Dordrecht: Springer Netherlands. https://doi.org/10.1007/978-94-017-0519-6_48

Ballantyne, A. P., Alden, C. B., Miller, J. B., Tans, P. P., & White, J. W. (2012). Increase in observed net carbon dioxide uptake by land and oceans during the past 50 years. *Nature*, *488*(7409), 70–72. https://doi.org/10.1038/nature11299

Beer, C., Reichstein, M., Tomelleri, E., Ciais, P., Jung, M., Carvalhais, N., et al. (2010). Terrestrial gross carbon dioxide uptake: Global distribution and covariation with climate. *Science*, *329*(5993), 834–838. https://doi.org/10.1126/science.1184984

Berg, A., Findell, K., Lintner, B., Giannini, A., Seneviratne, S. I., van den Hurk, B., et al. (2016). Land–atmosphere feedbacks amplify aridity increase over land under global warming. *Nature Climate Change*, *6*(9), 869–874. https://doi.org/10.1038/nclimate3029

Brienen, R. J., Phillips, O. L., Feldpausch, T. R., Gloor, E., Baker, T. R., Lloyd, J., et al. (2015). Long-term decline of the Amazon carbon sink. *Nature*, *519*(7543), 344–348. https://doi.org/10.1038/nature14283

Campbell, J. E., Berry, J. A., Seibt, U., Smith, S. J., Montzka, S. A., Launois, T., et al. (2017). Large historical growth in global terrestrial gross primary production. *Nature*, *544*(7648), 84–87. https://doi.org/10.1038/nature22030

Christoffersen, B. O., Gloor, M., Fauset, S., Fyllas, N. M., Galbraith, D. R., Baker, T. R., et al. (2016). Linking hydraulic traits to tropical forest function in a size-structured and trait-driven model (TFS v.1-hydro). *Geoscientific Model Development*, *9*(11), 4227–4255. https://doi.org/10.5194/gmd-9-4227-2016

Dai, A., Trenberth, K. E., & Qian, T. (2004). A global dataset of Palmer Drought Severity Index for 1870–2002: Relationship with soil moisture and effects of surface warming. *Journal of Hydrometeorology*, *5*(6), 1117–1130. https://doi.org/10.1175/JHM-386.1

Dirmeyer, P., Gao, X., & Oki, T. (2002). *The second global soil wetness project science and implementation plan, International GEWEX Project Office Publication Series* (Vol. 37, 75 pp.). IGPO.

Friedlingstein, P., Meinshausen, M., Arora, V. K., Jones, C. D., Anav, A., Liddicoat, S. K., & Knutti, R. (2014). Uncertainties in CMIP5 climate projections due to carbon cycle feedbacks. *Journal of Climate*, *27*(2), 511–526. https://doi.org/10.1175/JCLI-D-12-00579.1

Friend, A. D., Lucht, W., Rademacher, T. T., Keribin, R., Betts, R., Cadule, P., et al. (2014). Carbon residence time dominates uncertainty in terrestrial vegetation responses to future climate and atmospheric CO_2. *Proceedings of the National Academy of Sciences of the United States of America*, *111*(9), 3280–3285. https://doi.org/10.1073/pnas.1222477110

Huntingford, C., Zelazowski, P., Galbraith, D., Mercado, L. M., Sitch, S., Fisher, R., et al. (2013). Simulated resilience of tropical rainforests to CO_2-induced climate change. *Nature Geoscience*, *6*(4), 268–273. https://doi.org/10.1038/ngeo1741

Jackson, R. B., Canadell, J. G., Ehleringer, J. R., Mooney, H. A., Sala, O. E., & Schultz, E.-D. (1996). A global analysis of root distributions for terrestrial biomes. *Oecologia*, *108*(3), 389–411. https://doi.org/10.1007/BF00333714

Keeling, R. F., Graven, H. D., Welp, L. R., Resplandy, L., Bi, J., Piper, S. C., & Sun, Y. (2017). Atmospheric evidence for a global secular increase in carbon isotopic discrimination of land photosynthesis. *Proceedings of the National Academy of Sciences of the United States of America*, *114*(39), 10,361–10,366. https://doi.org/10.1073/pnas.1619240114

Lawrence, D. M., Slater, A. G., Romanovsky, V. E., & Nicolsky, D. J. (2008). Sensitivity of a model projection of near-surface permafrost degradation to soil column depth and representation of soil organic matter. *Journal of Geophysical Research*, *113*, F02011. https://doi.org/10.1029/2007JF000883

Le Quéré, C., Moriarty, R., Andrew, R. M., Peters, G. P., Ciais, P., Friedlingstein, P., et al. (2015). Global carbon budget 2014. *Earth System Science Data*, *7*(1), 47–85. https://doi.org/10.5194/essd-7-47-2015

Mankin, J. S., Smerdon, J. E., Cook, B. I., Williams, A. P., & Seager, R. (2017). The curious case of projected twenty-first-century drying but greening in the American West. *Journal of Climate*, *30*(21), 8689–8710. https://doi.org/10.1175/JCLI-D-17-0213.1

Mankin, J. S., Williams, A. P., Seager, R., Smerdon, J. E., & Horton, R. M. (2018). Blue water trade-offs with vegetation in a CO_2-enriched climate. *Geophysical Research Letters*, *45*, 3115–3125. https://doi.org/10.1002/2018GL077051

Milly, P. C. D., & Dunne, K. A. (2016). Potential evapotranspiration and continental drying. *Nature Climate Change*, *6*(10), 946–949. https://doi.org/10.1038/nclimate3046

Mystakidis, S., Davin, E. L., Gruber, N., & Seneviratne, S. I. (2016). Constraining future terrestrial carbon cycle projections using observation-based water and carbon flux estimates. *Global Change Biology*, *22*(6), 2198–2215. https://doi.org/10.1111/gcb.13217

Pan, Y., Birdsey, R. A., Fang, J., Houghton, R., Kauppi, P. E., Kurz, W. A., et al. (2011). A large and persistent carbon sink in the world's forests. *Science*, *333*(6045), 988–993. https://doi.org/10.1126/science.1201609

Poulter, B., Frank, D., Ciais, P., Myneni, R. B., Andela, N., Bi, J., et al. (2014). Contribution of semi-arid ecosystems to interannual variability of the global carbon cycle. *Nature*, *509*(7502), 600–603. https://doi.org/10.1038/nature13376

Powell, T. L., Galbraith, D. R., Christoffersen, B. O., Harper, A., Imbuzeiro, H. M., Rowland, L., et al. (2013). Confronting model predictions of carbon fluxes with measurements of Amazon forests subjected to experimental drought. *The New Phytologist*, *200*(2), 350–365. https://doi.org/10.1111/nph.12390

Roderick, M. L., Greve, P., & Farquhar, G. D. (2015). On the assessment of aridity with changes in atmospheric CO_2. *Water Resources Research*, *51*, 5450–5463. https://doi.org/10.1002/2015WR017031

Sanford, T., Frumhoff, P. C., Luers, A., & Gulledge, J. (2014). The climate policy narrative for a dangerously warming world. *Nature Climate Change*, *4*(3), 164–166. https://doi.org/10.1038/nclimate2148

Sato, H., Itoh, A., & Kohyama, T. (2007). SEIB–DGVM: A new dynamic global vegetation model using a spatially explicit individual-based approach. *Ecological Modelling*, *200*(3–4), 279–307. https://doi.org/10.1016/j.ecolmodel.2006.09.006

Sheffield, J., & Wood, E. F. (2007). Projected changes in drought occurrence under future global warming from multi-model, multi-scenario, IPCC AR4 simulations. *Climate Dynamics*, *31*(1), 79–105. https://doi.org/10.1007/s00382-007-0340-z

Shevliakova, E., Pacala, S. W., Malyshev, S., Hurtt, G. C., Milly, P. C. D., Caspersen, J. P., et al. (2009). Carbon cycling under 300 years of land use change: Importance of the secondary vegetation sink. *Global Biogeochemical Cycles*, *23*, GB2022. https://doi.org/10.1029/2007GB003176

Sitch, S., Friedlingstein, P., Gruber, N., Jones, S. D., Murray-Tortarolo, G., Ahlström, A., et al. (2015). Recent trends and drivers of regional sources and sinks of carbon dioxide. *Biogeosciences*, *12*(3), 653–679. https://doi.org/10.5194/bg-12-653-2015

Sperry, J. S., Venturas, M. D., Anderegg, W. R., Mencuccini, M., Mackay, D. S., Wang, Y., & Love, D. M. (2016). Predicting stomatal responses to the environment from the optimization of photosynthetic gain and hydraulic cost. *Plant, Cell & Environment*. https://doi.org/10.1111/pce.12852

Swann, A. L., Hoffman, F. M., Koven, C. D., & Randerson, J. T. (2016). Plant responses to increasing CO_2 reduce estimates of climate impacts on drought severity. *Proceedings of the National Academy of Sciences of the United States of America*. https://doi.org/10.1073/pnas.1604581113

Thornton, P. E., Lamarque, J.-F., Rosenbloom, N. A., & Mahowald, N. M. (2007). Influence of carbon-nitrogen cycle coupling on land model response to CO_2 fertilization and climate variability. *Global Biogeochemical Cycles*, *21*, GB4028. https://doi.org/10.1029/2006GB002868

Trenberth, K. E., Dai, A., van der Schrier, G., Jones, P. D., Barichivich, J., Briffa, K. R., & Sheffield, J. (2013). Global warming and changes in drought. *Nature Climate Change*, *4*(1), 17–22. https://doi.org/10.1038/nclimate2067

Trugman, A. T., Fenton, N. J., Bergeron, Y., Xu, X., Welp, L. R., & Medvigy, D. (2016). Climate, soil organic layer, and nitrogen jointly drive forest development after fire in the North American boreal zone. *Journal of Advances in Modeling Earth Systems*, *8*, 1180–1209. https://doi.org/10.1002/2015MS000576

Trugman, A. T., Medvigy, D., Anderegg, W. R. L., & Pacala, S. W. (2018). Differential declines in Alaskan boreal forest vitality related to climate and competition. *Global Change Biology*, *24*, 1097–1107. https://doi.org/10.1111/gcb.13952

van Mantgem, J. P., Stephenson, N. L., Byrne, J. C., Daniels, L. D., Franklin, J. F., Fulé, P. Z., et al. (2009). Widespread increase of tree mortality rates in the western United States. *Science*, *323*(5913), 521–524. https://doi.org/10.1126/science.1165000

Xu, X., Medvigy, D., Powers, J. S., Becknell, J. M., & Guan, K. (2016). Diversity in plant hydraulic traits explains seasonal and inter-annual variations of vegetation dynamics in seasonally dry tropical forests. *The New Phytologist*, *212*(1), 80–95. https://doi.org/10.1111/nph.14009

Zeng, X. (2001). Global vegetation root distribution for land modeling. *Journal of Hydrometeorology*, *2*(5), 525–530. https://doi.org/10.1175/1525-7541(2001)002<0525:GVRDFL>2.0.CO;2

Zhu, Z., Piao, S., Myneni, R. B., Huang, M., Zeng, Z., Canadell, J. G., et al. (2016). Greening of the Earth and its drivers. *Nature Climate Change*, *6*(8), 791–795. https://doi.org/10.1038/NCLIMATE3004